Physical and Mechanical Properties of Plasters Incorporating Aerogel Granules and Polypropylene Monofilament Fibres

Paul Westgate, Kevin Paine, Richard J Ball

BRE Centre for Innovative Construction Materials, Department of Architecture and Civil Engineering, University of Bath, Bath, BA2 7AY, UK

Abstract

Growing concern over global warming in recent years has required buildings to become significantly more energy efficient. One of the main ways of achieving this aim has been through the use of innovative materials to facilitate improvements in levels of building insulation. This paper describes the use of aerogel granules as an additive material for lime-based plasters, with the objective of improving the thermal efficiency of buildings whilst maintaining or improving vapour permeability.

Five experimental lime composite mixes were prepared, with lime putty as the binder material and aggregate comprising differing proportions of standard sand and aerogel granules. Previous work had already confirmed very low strengths for plaster mixes containing aerogel granules alone as the aggregate material; therefore, polypropylene fibres were incorporated as a secondary additive material to improve the mechanical properties and reduce strength loss attributed to shrinkage and cracking.

The flexural strength, compressive strength, thermal conductivity and water vapour permeability of lime composite mortars containing different volume fractions of aerogel were determined. Microstructures were examined using scanning electron microscopy and transmission electron microscopy. The results showed that aerogel granules can be successfully incorporated into lime plasters to improve thermal efficiency. The addition of aerogel was also found to improve moisture vapour permeability. The inclusion of polypropylene fibres in aerogel plasters was effective in reducing shrinkage and cracking to acceptable levels. Experimental mixes exhibited a slight reduction in strength

compared to standard plaster mixes, although this was compensated for by a high level of flexibility and toughness.

This work provides innovative information on utilising aerogel granules as an insulating plaster additive by addressing the issues of strength and flexibility, properties that are not normally associated with aerogel but which are of importance in a functional plaster material.

Key words: Aerogel, thermal insulation, nanomaterials, polypropylene fibres, insulating plaster

1. Introduction

Global warming continues to be one of the most challenging environmental problems we face today. Despite a growing number of climate change mitigation policies, total anthropogenic greenhouse gas emissions were the highest in history from 2000 to 2010 [1]. In the UK, the government is putting special emphasis on retrofitting and refurbishment of the existing housing stock in an effort to tackle this problem, as this offers the greatest potential for CO_2 reduction in the short to medium term. This will be an enormous challenge, with approximately 25 million homes requiring upgrading by the end of 2050 if carbon reduction targets are to be met [2]. One of the most promising ways in which buildings can be adapted to help meet these goals is through the use of state of the art insulation materials, and a highly insulating material in this respect is silica aerogel.

Aerogel is most often incorporated into buildings in the form of blankets for loft insulation or boards for wall and ceiling insulation. However, insulating boards can be wasteful of material due to the requirement to be cut to size. Also, insulating boards have the disadvantage of requiring a flat surface for fixing onto. As a solution to these limitations, several organisations are developing plaster mixes that incorporate aerogel in granular form. One experimental product developed by Stahl et al [3], comprised of a mineral and cement free binder and hydrophobised granular aerogel at up to 90% by volume, has achieved a thermal conductivity value of 0.025 W/mK. A similar composite material developed by Burrati et al [4] reportedly achieved a thermal conductivity value of 0.05 W/mK with 90% aerogel by volume; the equivalent material without aerogel had a value of 0.5 W/mK. To date, however, there is only one known commercially available plaster that incorporates aerogel granules as the insulating element: the Fixit 222 Aerogel Insulating Plaster System. Fixit 222 is a highly developed product, comprising aerogel granules, light weight mineral aggregate, natural hydraulic lime, white cement and calcium hydroxide. Despite the use of cement and mineral aggregate, it still claims to achieve a thermal conductivity value of 0.028 W/mK [5]. These new plasters have significantly better thermal insulation performance than

traditional cement or gypsum plasters with sand aggregate, which typically have thermal conductivity values of between 0.22 and 0.72 W/mK [6]. Interestingly, though, there appears to be no published information relating to strength or flexibility for any of these new insulating lime plaster materials. Two studies, involving cementitious mortars incorporating aerogel, which did investigate strength, reported compressive strength, flexural strength and thermal conductivity all reducing with increased aerogel content [7][8].

Aerogels are a special class of extremely low density, amorphous, mesoporous materials with a nanostructure. In the case of aerogels the 'nano' designation refers to the size of the pores within the material rather than the actual particle size. Pore sizes in aerogels are generally between 5 and 70 nm and have a pore density of between 85 and 99.8% by volume [9], resulting in a very low thermal conductivity, a low gaseous conductivity and a low radiative infrared transmission, making them an extremely efficient insulating material.

An important property of aerogel for use in construction materials is its behaviour in the presence of water. There are several methods of manufacturing an aerogel, and the method used determines whether the finished product is hydrophilic or hydrophobic. Hydrophilic aerogels possess a large number of surface hydroxyl groups, making them extremely hygroscopic. When liquid water enters the pore structure, the surface tension of the water exerts strong capillary forces on the pore walls, causing collapse. This problem can be easily solved, however, by converting the surface hydroxyl groups (-OH) to non-polar (-OR) groups, where R is typically a methyl group [10].

Aerogel possesses a very high strength to mass ratio and can support up to 1600 times its own mass [11]; however, as manufactured, it is a brittle material, having a fracture toughness of only ~0.8 kPa $m^{1/2}$. Although easily crushed, this does not destroy its porous structure; aerogel that has been ground into a powder occupies approximately the same space as the original sample, demonstrating that the pore structure of the material does not change significantly [12].

Initial attempts during this investigation to incorporate aerogel granules with lime plasters resulted in high shrinkage and extensive cracking of the lime matrix. This work seeks to mitigate these problems through the incorporation of monofilament polypropylene fibres. These fibres have been used extensively in cementitious building materials, and are considered one of the most effective methods to reduce plastic shrinkage and cracking in mortars [13]. The effects of the volume fraction of polypropylene fibre on the mechanical properties of concrete was investigated by Rajguru R. S. et al

[14]. It was found that the flexural strength of test beams increased significantly with increased fibre content from 0.25% to 0.5%, but the rate of strength increase achieved by increasing fibre content from 0.5% to 1% was marginal. Work has also been carried out to investigate ways of improving the mechanical properties of aerogel by incorporating fibres into the actual aerogel structure itself to produce fibre-reinforced aerogel composites. It was found that composites could be produced that had a higher strength compared to non-reinforced aerogel, but sacrificed little thermal performance [15].

Whilst aerogel may have the potential to help reduce energy usage in buildings, another important factor to consider in reducing carbon emissions is the embodied carbon of building materials. Non-hydraulic lime putty was used as the binder material for these experimental plaster mixes because it has a significantly lower environmental impact than that of the more commonly used Portland cement. Portland cement requires higher temperatures during production, and hence results in higher CO_2 output, than lime. But the case for lime as a low carbon material is strengthened further by the fact that it actually reabsorbs CO_2 whilst setting; a non-hydraulic lime putty can absorb nearly its own weight in CO_2 [16].

A further advantage of non-hydraulic lime is its long shelf life. It is common for manufacturers to recommend that, once opened, bags of lime are used within a specified time or discarded. In practice, practitioners may keep lime from a few days to one year depending on the storage conditions and risk of excessive hydration and carbonation within the bag. Non-hydraulic lime putty, however, can be stored for significantly longer due to the effectiveness of the milk-of-lime layer on the surface of the putty at preventing carbonation. The carbonation rate and plasticity of lime putty have been found to be still improving after periods in excess of five years [17].

The use of a lime putty as a binder is also advantageous for the recycling of materials. Hardened lime binder can be removed from masonry relatively easily, whereas the high strength bonding of cement mortars and renders can prevent recycling of materials, as it cannot be removed easily from brick and stone without causing damage.

An additional benefit to using lime is its superior water vapour permeability compared to modern commercial plasters [18]. When used as a render, the higher permeability of lime plaster helps moisture to escape from within the walls, preventing freeze thaw damage [19]. When used as a plastering material, its ability to release moisture helps to prevent mould formation and reduction in thermal resistance. Although there is little published data on the permeability of aerogel plasters, one study by

Ibrahim et al reported a figure of 5.1 x 10^{-11} kg/s m Pa for an experimental aerogel based external render [20]. This figure is significantly higher than was found in a study by Wang et al, where five commercially available gypsum plasters were found to achieve figures of between 1.62 and 2.53 kg/s m Pa [21].

Compared to other insulation materials such as glass and natural fibre, aerogel is still of higher cost. However, it should be noted that it is still a relatively new material for construction applications. As its use becomes more widespread, higher production quantities and economies of scale will help lower the cost [22]. Aerogel is the insulation material of choice for applications where the space available for insulation is limited but performance cannot be compromised. It is also noteworthy that over the service life of a building a reduction in operational costs associated with better insulation can be realised. Iddon and Firth (2013) report that for a typical building between 74-80% of the total energy in the first 60 years of service is consumed during operation and use. The remainder is the embodied energy and energy used during the construction process [23].

This paper investigates the use of granular aerogel incorporated into non-hydraulic lime-based plasters with the aim of developing a product that is highly insulating and has good vapour permeability, with the capability of reducing the operational energy consumption of buildings.

2. Experimental materials

2.1 Lime putty

The binder material used for this work was a lime putty supplied by J J Sharpe, which was matured for at least 6 months. The lime putty was weighed before and after drying in an oven to remove the water content and was found to have a solids content, assumed to be calcium hydroxide of 51%. This allowed accurate batching of the mix constituents.

2.2 Aerogel granules

The silica aerogel was supplied by Aerogel UK. The material comprises open cell, hydrophobic aerogel granules ranging in size from 125µm to 5mm.

2.3 Standard sand

The sand used in this investigation was a dry siliceous natural sand conforming to BS EN 196-1 and ISO 679: 2009. This grade of sand comprises particles that are generally isometric and rounded in shape and having a particle size distribution as shown in Figure 1. This type of sand was specified for this investigation to facilitate consistency and repeatability of experimental conditions.

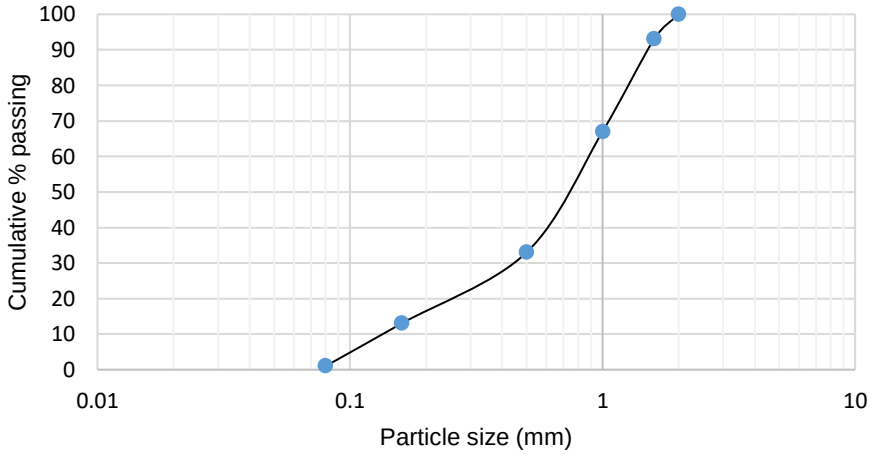

Figure 1: Particle size distribution for standard sand

2.4 Polypropylene fibres

Polypropylene monofilament fibres from Adfil [24] having lengths 12 and 18mm and a diameter of 20µm were added to the experimental plaster mixes at 0.5% by volume, to help reduce shrinkage and cracking. The fibres had been treated with a surfactant for optimum dispersion and bonding. No details of the surface treatment were provided by the manufacturer.

The volume fraction was kept at 0.5%, as it was considered that higher proportions of fibres might negatively affect the rheology of the plaster and that strength per se was not the most important physical property for a plaster.

2.5 Sample preparation

Five different plasters were prepared for testing using a mix ratio of 1:1 aggregate to lime putty by volume, giving a ratio ≈ 2:1 aggregate to lime by volume after allowing for the water content of the putty. The five specimens all contained fibres and varying ratios of aerogel and sand. The corresponding mix ratios and resulting bulk densities are presented in Table 1.

Table 1: Material composition by volume of experimental mixes

Specimen	Lime putty (%)	Standard sand (%)	Aerogel (%)	Polypropylene fibres (%)	Bulk density (kg/m^2)
S0	50	49.5	0	0.5	1,504
S1	50	37.25	12.25	0.5	1,294
S2	50	24.75	24.75	0.5	1,089
S3	50	12.25	37.25	0.5	883
S4	50	0	49.5	0.5	682

The lime and sand were prepared using a paddle mixer for a minimum of twenty minutes to ensure the plaster was suitably workable. Fibres were added to the mixture in small amounts during the mixing process to help ensure an even distribution throughout the matrix. The aerogel was added afterwards and mixed into the plaster by hand using a trowel. This was to avoid subjecting the aerogel to prolonged stress during mixing and possible degradation of the granules. The experimental mixes were then added to the prism moulds in small quantities and tamped down as the material was added, to reduce the occurrence of trapped air bubbles within the specimens. For each experimental mix, three standard 40x40x160mm prisms were prepared for strength testing, six discs of diameter 100mm and thickness 25mm for thermal conductivity testing and three discs of diameter 175mm and thickness 15mm for water vapour permeability testing.

After moulding, the specimens were stored in a climate chamber regulated at a constant temperature of 20ºC ± 2ºC and relative humidity of 65% ± 5% as specified in standard EN 1015-11:1999 [25]. The specimens were covered with a thin plastic wrap for the first week to maintain a high level of humidity, as exposure to ambient atmospheric conditions during this period can result in significant reduction in strength due to premature drying and subsequent cracking [26]. The specimens were then left in the moulds for a further week to allow them to achieve sufficient rigidity to facilitate demoulding.

3. Experimental methods

3.1 Strength testing

Mechanical strength testing was performed using a 50kN Instron 3369 Universal motorised load frame in accordance with BS EN 1015-11:1999 to test both the flexural and compressive strength. Bluehill 3 software monitored and recorded the load on the specimen as a function of extension throughout the test.

3.2 Electron microscopy

Scanning electron microscopy (SEM) was used to examine the physical condition of the specimens at the lime/aerogel interface to help identify any shrinkage around the aerogel particles or any degradation of the particles themselves. Specimens were analysed using a JEOL 6480 LV scanning electron microscope equipped with an Oxford Instruments INCA X-act X-ray detector (silicon drift detector offering high count rate and reduced operation time). High magnification images of the aerogel internal pore structure were obtained using a JEOL JEM1200EXII transmission electron microscope (TEM) operating at 120 kV.

3.3 Thermal conductivity measurement

Thermal conductivity measurements were obtained using the transient hot strip method. This method is suitable for thermal conductivity measurement of porous substances and has previously been used on plasters [27]. This method works by measuring the temperature rise at a known distance from a linear heat source. The linear heat source and the temperature sensor (thermocouple) are incorporated, at a known distance, within the sensing strip.

To take the measurements, the sensing strip was placed between two of the 100mm diameter disc specimens. The specimens were tested under normal conditions i.e. not dried. Upon commencing the measurement process, the apparatus heats up and establishes a stable temperature within the test specimens. Temperature data were recorded at two second intervals for a period of 120 seconds. The power setting for this test was 0.4 W. Measurements were repeated on three different pairs of specimen discs and an average value calculated for each mix.

3.4 Water vapour permeability testing

Water vapour permeability testing was carried out in accordance with BS EN 1015-19:1999. Three 175mm diameter specimens were tested for each of the five mixes. The discs were sealed onto the

open mouth of a circular test cell, which contained a 10 mm deep saturated solution of potassium nitrate, and the discs were sealed around their outside edge with silicon sealant. The air gap between the base of the specimen discs and the top of the saturated potassium nitrate solution was 10 mm (±1 mm). This experimental set up produced a relative humidity within the test cell (in the air gap between the top of the salt solution and the underside of the test specimen) of approximately 95% at 20°C.

Test samples were placed in a fan-assisted environmental chamber at 20ºC and 50% RH. A precision balance within the chamber logged the sample mass at five minute intervals on a PC. Monitoring was continued until a linear relationship between mass reduction and time could be established.

3.5 Fourier Transform Infra-Red Spectroscopy (FTIR)

FTIR was used to help identify any chemical reactions that may have taken place between the lime and the fibres or between the lime and the aerogel particles. FTIR spectra were obtained for the aerogel granules and the polypropylene fibres before and after they were added to the lime mixes. A PerkinElmer Frontier FTIR spectrometer was used over a frequency range from 600 – 4000 cm^{-1} and at a resolution of 1 cm^{-1} and 40 accumulations.

4. Results

4.1 Compressive and flexural strength

Figures 2 and 3 show stress as a function of strain during compressive and flexural testing respectively. The data was reported up to a strain value of 0.03 as a consequence of the failure mode behaviour of specimens containing fibres. At higher values of strain the test data indicates that the specimens did not fail in a brittle manner even though their condition was such that they would have been considered to have failed as a building element.

As the flexural test caused test specimen deformation but did not fracture it, the deformed specimen was manually broken in half after the test, and fibres and binder were removed from the fracture faces for further testing.

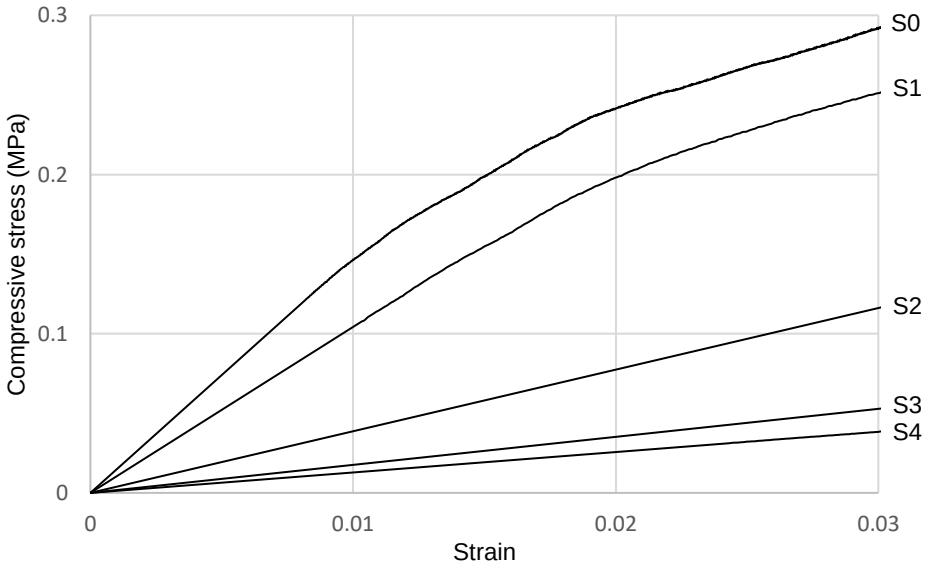

Figure 2: Average compressive strength test results for each of the five plasters

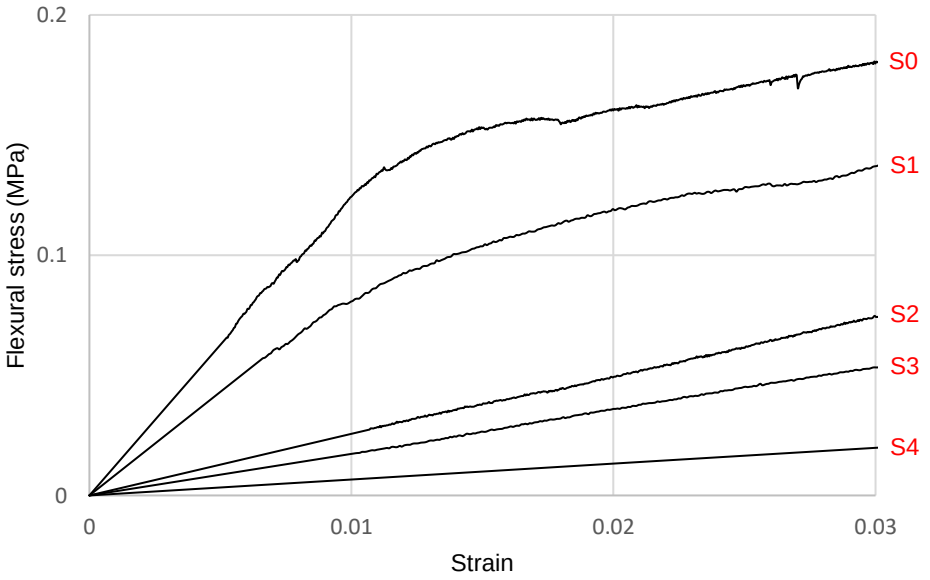

Figure 3: Average flexural strength test results for each of the five plasters

4.2 Effect of fibres on failure mode

Figure 4 shows the different behaviours under stress of lime mortars with and without fibres added. Figure 4 (A) shows a typical behaviour for a standard lime mortar (without fibres) under compression. At failure, the specimen fractures and fails at a distinct point in the test. In Figure 4 (B) it can be seen from the degree of compression at the base of a specimen containing aerogel (S1) that the addition of 0.5% fibres by mass permits the lime mortar to achieve a high strain capacity, and that the fibres have prevented fracturing and have helped to maintain the integrity of the specimen.

Similarly, during flexural testing a significant difference is observed between the specimens with and without fibres added. The standard mix lime specimen cracked at the point of maximum stress (Figure 5 (A) and broke into two halves. Figure 5 (B) shows that the specimen containing fibres endured a significantly higher strain without failing and has considerably greater flexibility.

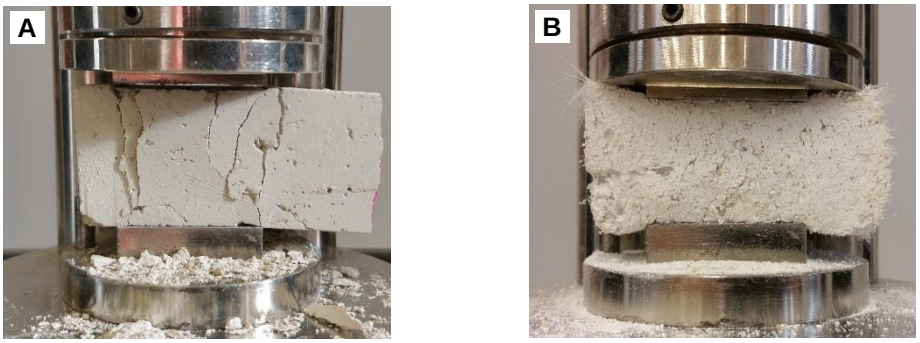

Figure 4: Compressive fracture of a reference mortar without fibres (A) and typical deformation of a specimen (S1) containing fibres and aerogel (B)

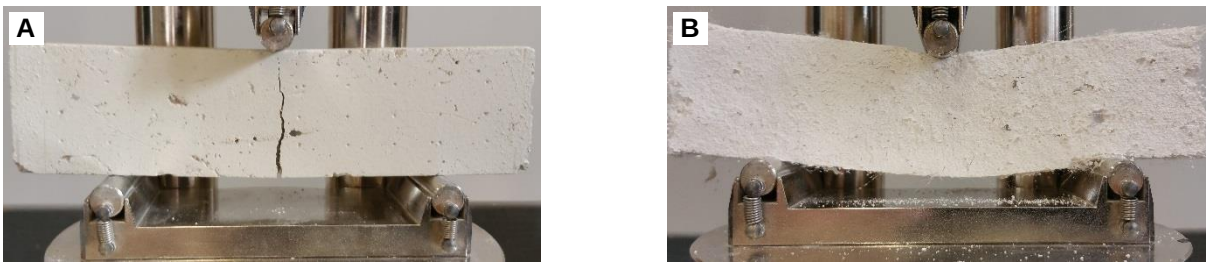

Figure 5: Flexural fracture of reference mortar without fibres (A) and deflection of a specimen (S1) containing fibres and aerogel (B)

4.3 Scanning electron microscopy (SEM)

It can be seen that the typical morphology of the aerogel granules was an irregular shape and this contained different features including both smooth and rounded surfaces in addition to some sharper edges (Figure 6).

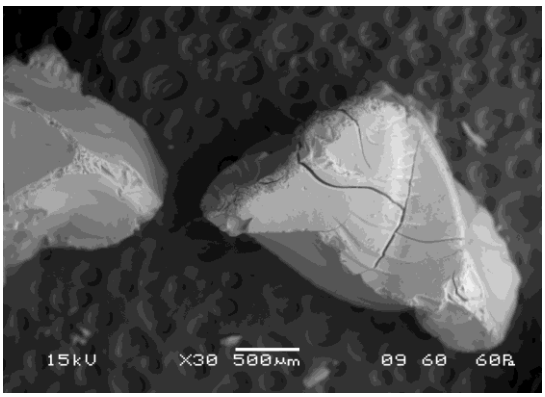

Figure 6: Aerogel particles as manufactured

The images in Figure 7 (A) and (B) show aerogel particles in a specimen after 91 days. Figure 7 (A) shows a particle embedded in the binder, which has remained intact and not deteriorated in any discernible way. In Figure 7 (B) it can be seen that there is no evidence of shrinkage at the aerogel/ lime interface. This finding is consistent with a study by Gao, T. et all, which reported that aerogel particles in 'aerogel incorporated concrete' survive the mixing and curing process without suffering degradation [28]. The images in Figure 8 (A) and (B) show the effect of the binder on the surface of the fibres. In Figure 8 (A), damage to the fibre surface is clearly visible in the form of scratches along the length of the fibre. This fibre was extracted from the fracture face of a test prism after flexural strength testing, and the marking was caused by the fibres being pulled with force from the binder matrix during the test. For reference, Figure 8 (B) shows the smooth and unmarked surface of a fibre in its original unused condition. Figure 9 (A) and (B) shows images of plaster particles removed from the fracture face of a test specimen. In Figure 9 (A), it can be seen that these particles have suffered physical stress, as the aerogel particles have fractured and appear as shards. In Figure 9 (B), the aerogel particle appears to have remained intact. In both cases, binder remains adhered to the aerogel. In Figure 10 (A) and (B), evidence of the bond between the lime binder and the fibres is visible. These fibres were pulled from the specimen matrix, yet calcite crystals remain firmly attached to the fibres indicating a strong bond.

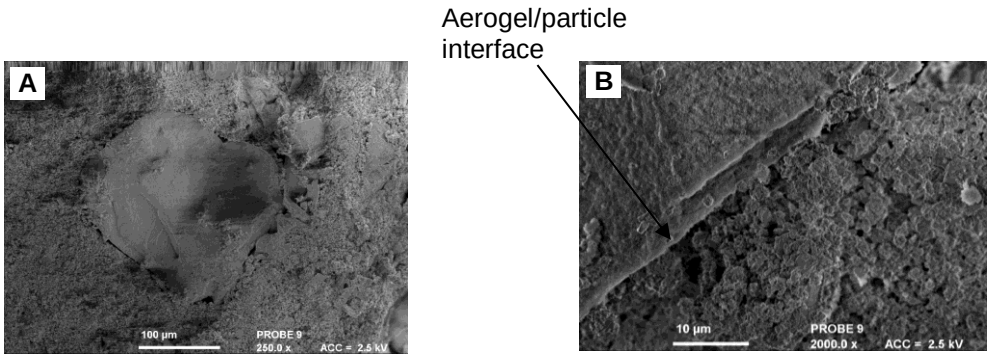

Figure 7: Aerogel particle in lime binder after 91 days (image A). Aerogel/lime interface (image B).

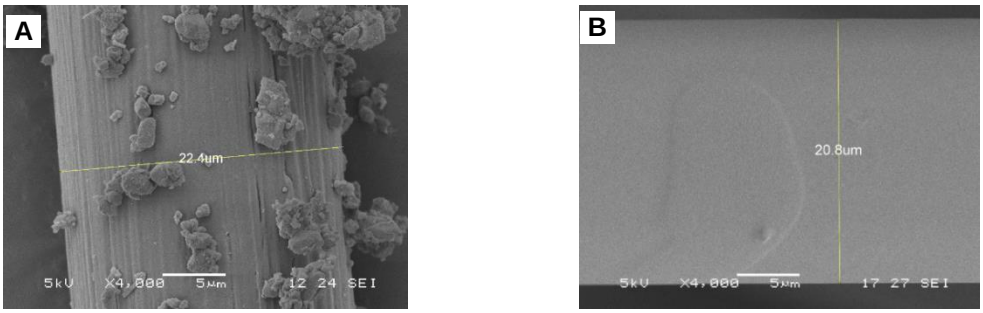

Figure 8: Fibre extracted from fracture surface of test specimen (image A). Fibre in as manufactured condition (image B).

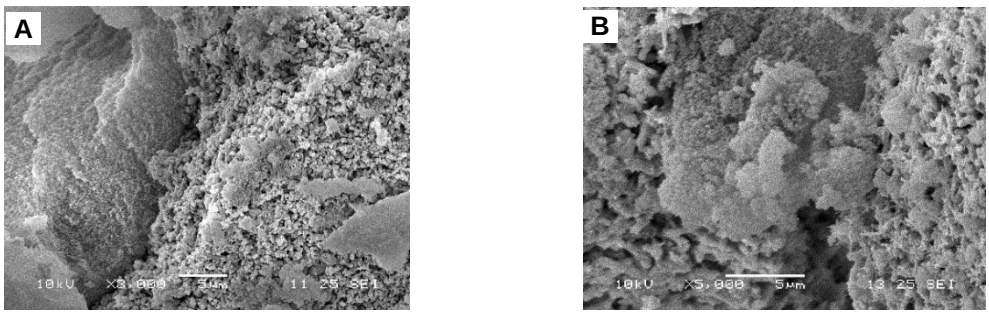

Figure 9: Calcite crystals adhering to aerogel particles (image A). Aerogel particle entrapped within calcite (Image B).

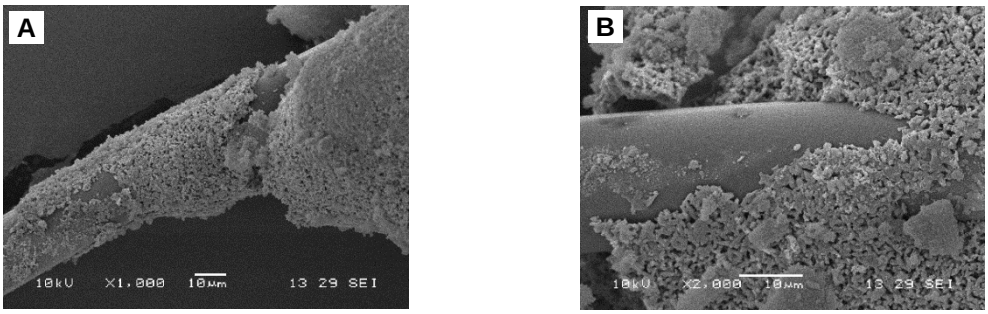

Figure 10: Calcite crystals adhering to the surface of a polypropylene fibre (image A). Fibre/binder interface (image B).

4.4 Transmission electron microscopy (TEM)

A crushed aerogel particle was examined using TEM. The image in Figure 11 shows the mesoporous nature of the internal structure, which is the physical property that is responsible for the low conductive and gaseous heat transfer through the material. Accurate measurement of the pore and pore wall dimensions was beyond the capability of the equipment.

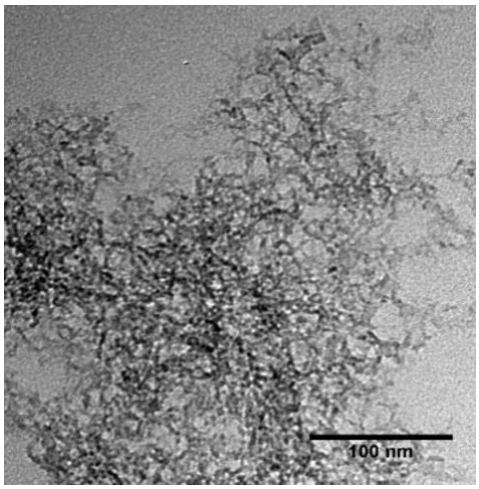

Figure 11: TEM image of a crushed aerogel particle showing the highly porous nature of its internal structure. (Magnification = 250,000x)

4.5 Thermal conductivity

Figure 12 shows the thermal conductivity for each experimental mix. To provide statistically significant results, an average of three separate test runs using a different pair of specimens for each test is reported. The thermal conductivity decreased significantly with increased aerogel content.

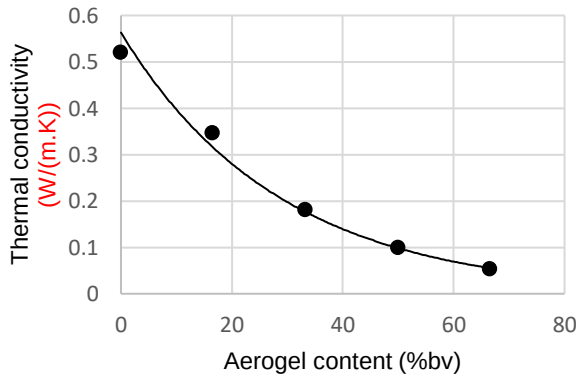

Figure 12: Effect of aerogel content on thermal conductivity

Thermal conductivity values as a function of aerogel content by volume show an exponential relationship as per equation 3 where, λ is thermal conductivity, Ae is aerogel content and k is the rate of change.

$$\lambda_{(Ae)} = \lambda_{(0)} e^{k \cdot Ae} \qquad (3)$$

Using a value of 66.6 for Ae gives a value of -0.03428 for k. This exponential relationship can be explained by the fact that as the volume fraction of low density aerogel was increased, the volume fraction of high density quartz sand was decreased proportionally. The thermal insulating performance of the plaster mix comprising only aerogel as aggregate (S4) was only marginally inferior to other experimental insulating plasters being developed using aerogel; however, the plaster mixes investigated here utilised a significantly lower proportion of aerogel compared to those materials developed by Stahl et al [3] and Burrati et al [4].

4.6 Water vapour permeability

Figure 13 shows the weight loss data for each specimen measured over a period of ten hours. The data, when plotted, shows a linear relationship between time elapsed and weight of moisture lost by diffusion through the specimen under test. The permeability clearly increased with higher aerogel content and remained constant throughout the test. This tendency was attributed to the hydrophobicity of the aerogel preventing the blockage of the pores with moisture.

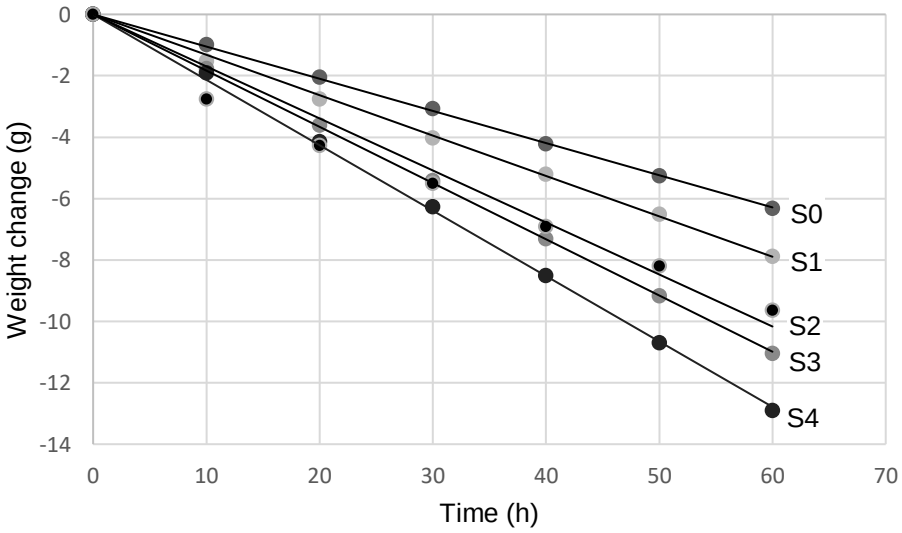

Figure 13 Graph of weight loss against time during wet cup permeability test

The weight loss data from the wet cup test allowed calculation of the water vapour permeance and water vapour permeability values (Figure 14) for each mix, using formulae (1) and (2) below.

$$W_{vp} = \Lambda t \qquad (1)$$

$$\Lambda = \frac{1}{A\Delta_p/(\Delta G/\Delta t) - R_A} \qquad (2)$$

Where: W_{vp} is water vapour permeability (kg m^{-1} s^{-1} Pa^{-1}), Λ is water vapour permeance (kg m^{-2} s^{-1} Pa^{-1}), A is area of open mouth of test cell (m^2), D_p is the difference in water vapour pressure between ambient air and potassium KNO_3 solution (Pa), R_A is water vapour resistance of air gap between specimen and KNO_3 solution (0,048 x 10^9 Pa m^2s/kg per 10 mm air gap), DG/Dt is the water vapour flux (kg/s), and t is specimen thickness (m).

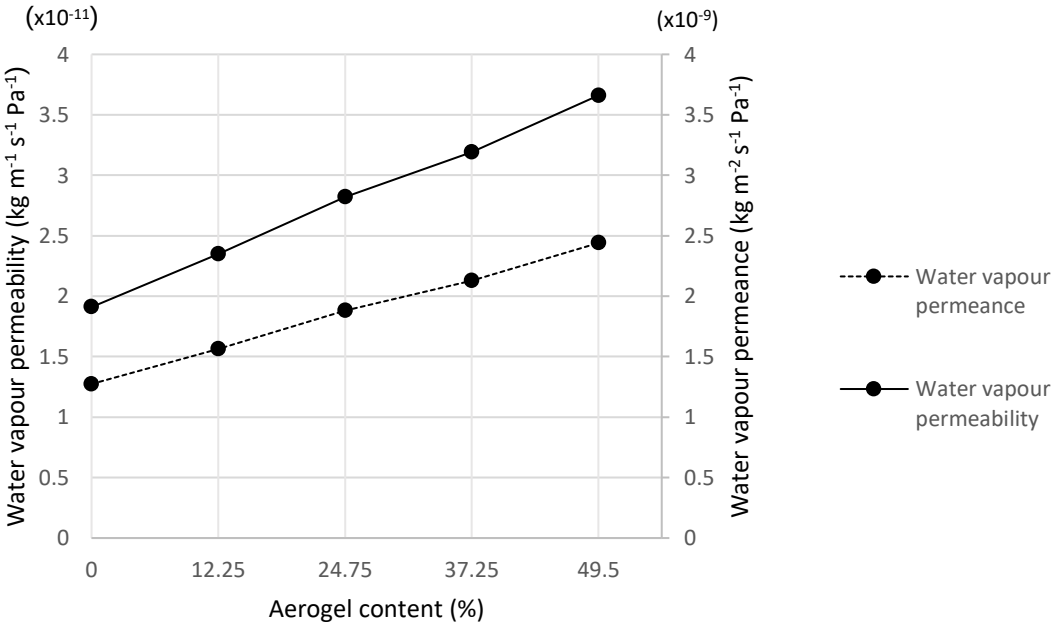

Figure 14: Aerogel effect on water vapour permeability

4.7 FTIR

Figures 15(A) and 15(B) show spectra for aerogel obtained from a test specimen and from aerogel as manufactured respectively. The aerogel specimen exhibited a main absorption peak at 1083 cm^{-1}, with a shoulder at around 1200 cm^{-1}, which is characteristic of silica and can be assigned to asymmetric Si-O-Si stretching vibrations [29]. A second peak at 949 cm^{-1} is assigned to silanol (Si-OH) stretching vibrations, indicating that the aerogel is not 100% hydrophobic. An additional characteristic silica Si-O-Si stretching peak was observed at 800 cm^{-1}. [30]. The peak at 847 cm^{-1} is assigned to Si-CH_3 rocking vibrations in silanes and is consistent with surface methyl groups produced during hydrophobization [31].

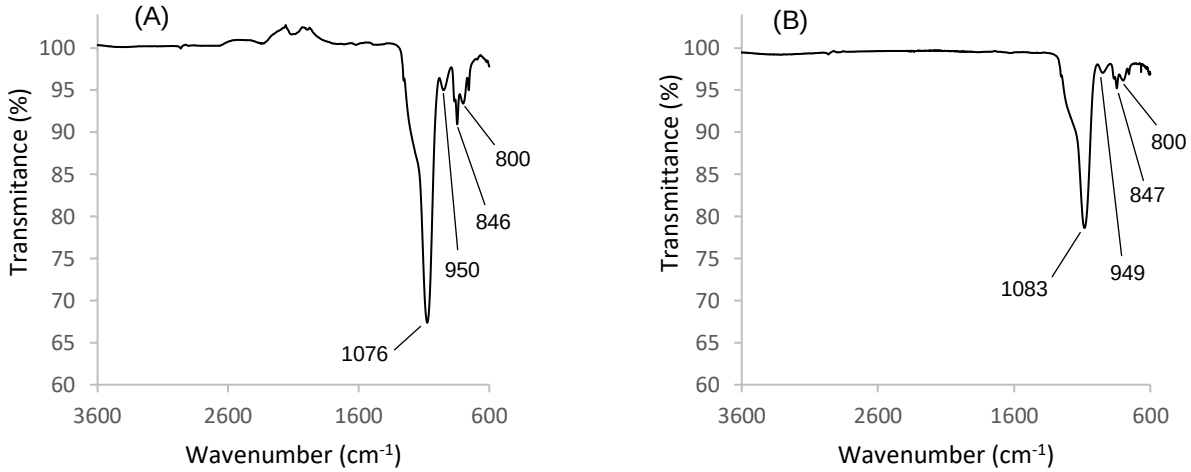

Figure 15: FTIR spectra of aerogel taken from test specimen (A) and from aerogel as manufactured (B).

Figures 16 (A) and 16(B) show spectra for a fibre obtained from a test specimen and from a fibre as manufactured respectively. The spectrum obtained from the polypropylene fibre was a match on all the main peaks with the reference polypropylene spectrum [32], but there were no significant additional peaks to provide information on the surface treatment. This suggests that the surfactant used on the fibres was an extremely thin surface layer and below the instrument's detection limit.

For both the aerogel and the polypropylene fibres, the absence of any significant difference between the FTIR spectra before and after they had been in contact with the lime binder is consistent with no chemical reaction having taken place between the binder and the additive materials. This supports the evidence from the SEM images indicating that the strength gain from the incorporation of fibres is the result of a physical rather than chemical bond.

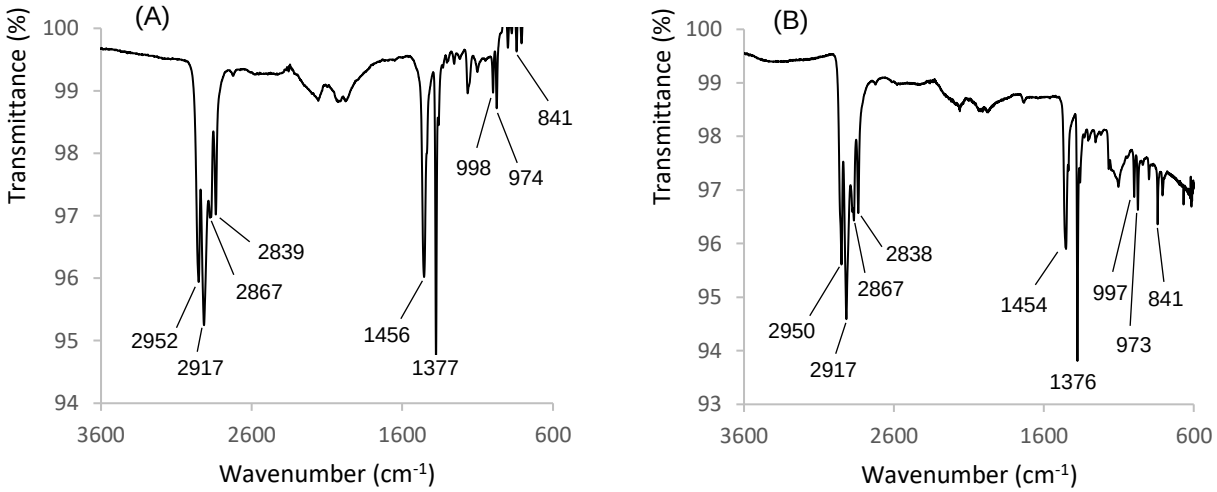

Figure 16: FTIR spectrum of polypropylene fibre taken from test specimen (A) and from a polypropylene fibre as manufactured (B).

4. Discussion

Whilst the inclusion of aerogel clearly improves the thermal efficiency of the plaster mixes, the only specimen that achieved thermal efficiency comparable to similar aerogel plasters currently reported in the literature was the specimen comprising purely aerogel as the aggregate material (S4). When sand is incorporated into the mix, thermal conductivity rises significantly due to its high density compared to the aerogel. It should be taken into consideration, however, that the proportions of aerogel used in these experimental mixes was lower than those used in the other studies.

As initial attempts at incorporating aerogel into lime binders produced plasters that suffered shrinkage, cracking and very low strength, it is interesting that other similar investigations have not reported data for compressive and flexural strength. The strength values obtained during this investigation, even with fibres added to the binder, were significantly lower than that which would normally be expected for a lime plaster. However, the high degree of plastic deformation without fracturing demonstrated the superior flexibility and toughness of these experimental mixes in comparison to the more commonly used lime/sand mixes without added fibres. These experimental mixes clearly sacrifice strength for flexibility and toughness, but for a plaster, this can be a distinct advantage because the plaster can accommodate building movement, which helps to avoid cracking.

The specimen comprising only aerogel as the aggregate material exhibited permeability significantly superior to conventional gypsum plasters and comparable to a similar developmental aerogel product. This effect can clearly be attributed to the aerogel. The linear relationship between permeability and

aerogel content indicates that changes in the sand proportions had a negligible effect on permeability compared to changes in the aerogel content. This is of particular benefit when using non-hydraulic lime, which sets purely through carbonation and depends on the pore structure of the plaster for diffusion of CO_2. This property of aerogel containing plasters is also beneficial to the 'breathability' of a building, as it can assist the release of moisture absorbed by walls that could otherwise freeze and expand, causing damage to masonry.

The SEM images obtained from the polypropylene fibres support the assumption that they are responsible for imparting flexibility to the plaster. The surface of the new polypropylene fibre is clearly very smooth; however, the surface condition of fibres extracted from the fracture face of test specimens shows score marks along the length of the fibre, which is consistent with there being a physical bond between the binder and the fibres. The nature of the surface damage to the fibres is consistent with the gradual failure mode observed during strength testing, whereby the physical bond between binder and fibres provides resistance to pull-out and hence improved plastic deformation. It is also evident from the measurements taken from these images that the fibres are not stretching and thinning under tension. The absence of any evidence of chemical bonding between the lime and fibres, and the nature of the linear marking along the axis of fibres extracted from test specimens, is also consistent with resistance to fibre pull-out being responsible for the high levels of flexibility.

The low strength and rough surface texture (Figure 4b) of these experimental mixes would not make this a practical choice for a surface plaster coat. However, they could be utilised as the first coat in a multi-coat plaster. Traditionally, the first coat is the thickest, which would be the ideal location for incorporation of the aerogel plaster. The subsequent top coats would then provide the required protection and quality of finish.

The number of permutations of different mixes using the materials considered here is vast and beyond the scope of one study. There exists, therefore, significant scope for further work in this area, specifically the investigation of different binder to aggregate ratios, volume fraction and types of fibres and volumetric proportions of aerogel.

5. Conclusions

- The results of this investigation confirm that aerogel granules can be successfully incorporated into non hydraulic lime putty to produce viable lightweight, thermally insulating plasters.

- The thermal performance and permeability of the plaster containing only aerogel aggregate was superior to conventional plasters on the market and comparable to similar aerogel based insulating plasters being developed that contain higher proportions of aerogel.
- Previous investigations into aerogel based plasters have not considered strength or flexibility, which are important factors for in service use. The viability of the plasters developed in this investigation was strongly dependent on the inclusion of fibres, which improved flexibility and toughness and reduced shrinkage and cracking.
- The use of aerogel insulating plaster
- There is considerable scope for further work by investigating different mix proportions and different specification materials.

Acknowledgements

We thank Chris Meyer at Singleton Birch and Joe Orsi of Orsi Contini Consultants for their help in supplying materials and helpful advice.

References

[1] IPCC, 2014. Edenhofer, O., R. Pichs-Madruga, Y. Sokona, E. Farahani, S. Kadner, K. Seyboth, A. Adler, I. Baum, S. Brunner, P. Eickemeier, B. Kriemann, J. Savolainen, S. Schlömer, C. von Stechow, T. Zwickel and J.C. Minx (eds.)., 2014. Climate Change 2014: Mitigation of Climate Change. *Contribution of Working Group III to the Fifth Assessment Report of the Intergovernmental Panel on Climate Change*. Cambridge University Press, Cambridge, United Kingdom and New York, NY, USA, p.6.

[2] Edwards, J & Townsend, A., 2011. Buildings under Refurbishment. *Carbon Action 2050 White Paper.* Chartered Institute of Building: Englemere

[3] Stahl, S., Brunner, S., Zimmermann, M., Ghazi Wakili, K., 2012. Thermo-hygric properties of a newly developed aerogel based insulation rendering for both exterior and interior applications, *Energy and Buildings,* 44(2012), pp.114-117

[4] Buratti, C., Moretti, E., Belloni, E., and Agosti, F., 2014. Development of Innovative Aerogel Based Plasters: Preliminary Thermal and Acoustic Performance Evaluation. *Sustainability*, 6, pp.5839-5852

[5] Fixit, 2016. *Aerogel Insulating Plaster System* [online]. Available from:

http://www.fixit.ch/aerogel/pdf/Fixit_222_Aerogel_Verarbeitungsrichtlinien_A4_EN.pdf [accessed 7 August 2016].

[6] The Engineer, 2006. Thermal Conductivity, *The Engineer,* October 2006

[7] Ng, S., Jelle, B. P., Zhen, Y., Wallevik, O, H., 2016. Effect of storage and curing conditions at elevated temperatures on aerogel-incorporated mortar samples based on UHPC recipe. *Construction and Building Materials,* 106(2016), p.645.

[8] Julio, M. F., Soares, A., Ilharco, L. M., Flores-Cohen, I., Brito, J., 2016. Aerogel-based renders with lightweight aggregates: Correlation between molecular/pore structure and performance. *Construction and Building Materials,* 124(2016) p.493

[9] Baetens, R., Jelle, B.P. and Gustavsen, A., 2011. Aerogel insulation for building applications: A state of the art review. *Energy and buildings*, 43(4), p.764.

[10] Ayers, M., 2016. *Science of aerogels* [online]. California: E. O. Lawrence Berkely National Laboratory. Available from: http://energy.lbl.gov/ecs/aerogels/sa-chemistry.html [accessed 9th May 2016.

[11] Haranath, D., 1996. Aerogel The Lightest Solid Known. *Resonance,* November 1996, p.64.

[12] Kistler, S.S., 1931. Coherent expanded aerogels. *The Journal of Physical Chemistry*, 01/1931, Vol.36(1), pp.58.

[13] Filho, R.D., Toledo, Sanjuan, M.A., 1999. Effect of low modulus sisal and polypropylene fibre on the free and restrained shrinkage of mortars at an early age. *Cement and Concrete Research,* 1999, Vol.29(10), pp.1597.

[14] Rajguru, R. S., Ghode A. R., Pathan M. G., Rathi M. K., 2014. Effect of volume fraction of polypropylene fiber on the mechanical properties of concrete, *Int. Journal of Engineering Research and Applications, Vol. 4, Issue 6(Version 1), June 2014,* pp.67-69

[15] Yang, X., Sun, Y., Shi, D., Liu, J., 2011. Experimental investigation on mechanical properties of a fiber-reinforced silica aerogel composite. *Materials Science and Engineering A*, 528 pp.4830–4836

[16] Greenspec, 2017, *Lime mortar, render and plaster* [online]. Available from: http://www.greenspec.co.uk/building-design/lime-mortar-render/ [acessed 18th January 2017].

[17] Margalha, M. G., Silva, A. S., Do Rosário Veiga, M., De Brito, J., Ball, R. J. and Allen, G. C., 2013. Microstructural changes of lime putty during aging. *Journal of Materials in Civil*

Engineering, 25 (10), pp. 1524-1532.

[18] Straube, J., 2000. Moisture Properties of Plaster and Stucco for Strawbale Buildings, *Research Highlight,* Technical Series 00-132, p.3

[19] El-Turki, A., Ball, R. J., Holmes, S., Allen, W. J. and Allen, G. C., 2010. Environmental cycling and laboratory testing to evaluate the significance of moisture control for lime mortars. *Construction and Building Materials*, 24 (8), pp. 1392-1397.

[20] Ibrahim M., Wurtz, E., Biwole, P. H., Achard, P., Sallee, H., 2014. Hygrothermal performance of exterior walls covered with aerogel-based insulating rendering. *Energy and Buildings,* 84 (2014) p.243

[21] Wang, Q., Liu, H., 2011. The Experimental Research on the Water Vapour Permeability of Construction Gypsum Plaster Materials. *International Conference on Materials for Renewable Energy & Environment,* May 2011, Vol. 1, pp.854

[22] Ibrahim, M., Biwole, P. H., Achard, P. & Wurtz, E., 2015. Aerogel-based Materials for Improving the Building Envelope's Thermal Behaviour: A Brief Review with a focus on a New Aerogel-Based Rendering, *Energy Sustainability Through Green Energy*. New Delhi Heidelberg New York Dordrecht London: Springer, p.186

[23] Iddon, C. R. & Firth, S. K. 2013. Embodied and operational energy for new-build housing: A case study of construction methods in the UK. *Energy and Buildings*, 67 (2013), p.479

[24] Adfil, 2016. *Monofilament fibres* [online]. Available from: http://adfil.co.uk/products/micro-synthetic-fibres/monofilament-fibres/ [accessed 12th May 2016].

[25] EN 1015-11:1999. *Methods of test for mortar for masonry - Part 11: Determination of flexural and compressive strength of hardened mortar.* BSI

[26] Livesey, P., 2010. The Use of Lime Mortars and Renders in Extreme Weather Conditions. *Journal of the Building Limes Forum,* 17, 2010, pp.46-49

[27] Singh, R., 1984. Simultaneous measurement of thermal conductivity and thermal diffusivity of some building materials using the transient hot strip method, J. Phys. D: Appl. Phys.. 18, p.1

[28] Gao, T., Jelle, B. P., Gustavsen, A., Jacobsen, S., 2014. Aerogel-incorporated concrete: An experimental study. *Construction and Building Materials,* 52(2014), p.132

[29] Innocenzi, P., 2003. Infrared spectroscopy of sol–gel derived silica-based films: a spectra-microstructure overview. *Journal of Non-Crystalline Solids,* 316 (2003) 309–319, pp. 311-313

[30] Swann, G.E.A., and Patwardhan, S.V., 2011. Application of Fourier Transform Infrared Spectroscopy (FTIR) for assessing biogenic silica sample purity in geochemical analyses and palaeoenvironmental research. *Climate of the Past,* 7, 65–74, p.67

[31] Lambert, J.B., 1987. *Introduction to Organic Spectroscopy.* USA: Macmillan, p.176

[32] NICODOM, 2012. *FTIR Spectra of Polymers* [online]. Nicodom s.r.o.: Czech Republic. Available from: http://www.ftir-polymers.com/soon.htm [accessed: 15th May 2016